PROSPECT - A Precision Reactor Neutrino and Oscillation Spectrum Experiment at Very Short Baselines

Z. Djurcic
Argonne National Laboratory, Argonne, IL 60439

S. Hans and M. Yeh
Chemistry Department, Brookhaven National Laboratory, Upton, NY 11973

E. Blucher
Physics Department, University of Chicago, Chicago, IL 60637

R. Johnson and B.R. Littlejohn
Physics Department, University of Cincinnati, Cincinnati, OH 45221

M. Dolinski and C. Lane
Physics Department, Drexel University, Philadelphia, PA 19104-2875

T. Allen and S. Morrell
ATR National Scientific User Facility, Idaho National Laboratory, Idaho Falls, ID 83401

J.G. Learned and J. Maricic
University of Hawaii, Honolulu, Hawaii 96822

A. Bernstein, N.S. Bowden, T. Classen, A. Glenn, and N. Zaitseva
Physics Division, Lawrence Livermore National Laboratory, Livermore, CA 94550

H.P. Mumm, J.S. Nico, and R.E. Williams
National Institute of Standards and Technology, Gaithersburg, MD 20899

R. Henning
Department of Physics and Astronomy, University of North Carolina, Chapel Hill, NC 27599 and Triangle Universities Nuclear Laboratory, Durham NC 27710

C. Bryan, D. Dean, Y. Efremenko, and D. Radford
Oak Ridge National Laboratory, Oak Ridge, TN 37831

P. Huber, J.M. Link, and C .Mariani
Center for Neutrino Physics, Virginia Tech, Blacksburg, VA 24061

A.B. Balantekin, H.R. Band, J.C. Cherwinka, and K.M. Heeger
Physics Department, University of Wisconsin, Madison, WI 53706

W. Wang
Department of Physics, College of William and Mary, Williamsburg, VA 23187

K.M. Heeger and T. Langford
Department of Physics, Yale University, New Haven, CT 06520

(The Short-Baseline Reactor Neutrino Experiment Interest Group)

(Dated: October 1, 2013)

Antineutrino detectors operated close to a compact research reactor can provide excellent sensitivity to short-baseline oscillation effects through a precision measurement of the reactor antineutrino spectrum at various distances from the core. We describe a proposed 2-detector experiment with a baseline of 4-20m that will enable a high-precision measurement of the reactor antineutrino spectrum from a highly-enriched uranium core at a US research reactor and provide a definitive search for short-baseline neutrino oscillations. In addition, this experiment will provide important enabling technology for reactor monitoring applications.

PACS numbers: 14.60.Pq

I. INTRODUCTION

Reactor neutrino experiments have played an important role throughout the history of neutrino physics and led to many of the key discoveries in the field. From the first experimental observation of the antineutrino by Reines and Cowan at Savannah River, to the discovery of reactor electron antineutrino disappearance by KamLAND and the recent measurement of the neutrino mixing angle θ_{13} by Daya Bay, Double Chooz, and RENO, experiments with reactor antineutrinos have provided key insight into the nature of neutrinos. Together, the recent discoveries of neutrino flavor change in reactor, solar, and accelerator experiments have established the new Standard Model of 3-flavor neutrino oscillation.

Anomalous results from a variety of short-baseline experiments do not fit this framework and have challenged the global 3-flavor interpretation of neutrino and antineutrino data. This includes anomalous event excesses in $\overline{\nu}_e$ and ν_e appearance channels [1, 2], deficits in observed events in solar neutrino detector calibrations with high-intensity ν_e sources [3], and preference for more than three neutrino species in astrophysical surveys [4, 5]. Most recently, a re-analysis of short-baseline reactor neutrino experiments has revealed a discrepancy between observations and the predicted antineutrino flux. While the spectral shape and uncertainties obtained in this work are comparable to previous predictions, the predicted reactor $\overline{\nu}_e$ flux has increased by about 3.5% [6–8]. When combined with experimental data at baselines between 10-100 m these recent calculations suggest a $\sim$5.7% difference between the measured and predicted reactor antineutrino flux.

This "reactor anomaly" can be interpreted as either a sign of new physics or due to unknown physics in the reactor $\overline{\nu}_e$ flux predictions. It has been suggested that such a deficit may be the signature of additional sterile neutrino states with mass splittings of the order of $\sim 1\text{eV}^2$ and oscillation lengths of $\mathcal{O}(3\,\text{m})$ [3]. Additional sterile neutrino mass states with $\Delta m^2 \sim 1$ eV^2 beyond the 3 active neutrinos would yield an oscillation effect for $\overline{\nu}_e$ traveling over meter-long baselines from a finite-sized reactor core to a finite-sized detector. Experiments capable of testing the suggested oscillation at high statistical significance are necessary to definitively address the sterile neutrino hypothesis [9].

Current km-scale reactor experiments, while highly precise, cannot easily probe oscillation lengths of this order [10–12]. At these baselines the oscillation effect from potential sterile states averages to yield an effective rate deficit. Most existing experiments are limited by the contributions from multiple reactor cores and an inability to take background data without the presence of any reactor $\overline{\nu}_e$. A new experiment at very short baselines in a controlled research environment is needed to fully disentangle reactor flux and spectrum uncertainties from possible sterile neutrino oscillations and other effects.

One experimental approach [9, 13] is to measure the reactor $\overline{\nu}_e$ flux and spectrum from reactors at distances comparable to the expected sterile neutrino oscillation length of $\mathcal{O}(3\,\text{m})$. A measurement of the $\overline{\nu}_e$ energy spectrum as a function of distance can be used to perform a definitive search for oscillations in the region suggested by global fits. However, at these short baselines, a detector's position resolution, energy resolution, and the finite dimensions of the reactor core become important. This motivates the use of segmented detectors [14] near reactors with compact cores (dimensions of <1 m). The use of highly-enriched uranium (HEU) fuel in US research reactors offers a unique, very nearly static, core composition that minimizes spectral variations during oscillation measurements and will help test our understanding of reactor $\overline{\nu}_e$ calculations. A benchmark measurement of a static core will also provide the opportunity to better understand the time variation of $\overline{\nu}_e$ spectra at conventional reactors with low-enriched uranium (LEU) fuel. The duty cycle of research reactors provides an opportunity for extensive background measurements during the duration of the experiment. Fuel handling at research reactor facilities may enable dedicated studies of spent nuclear fuel that are not possible at commercial power plants.

Experimental challenges including the background rejection in detectors operated near a reactor and without significant overburden, the precision energy calibration, and control of detector systematics are tractable with existing technologies and the recent experience from multi-detector $\overline{\nu}_e$ experiments [11, 12]. Careful detector and shielding designs will be required and can be validated in R&D at the reactor sites. Multiple, segmented detectors with position resolution will allow a relative measurement of the $\overline{\nu}_e$ flux and spectrum at different distances.

Until recently the principal driver of very-short baseline reactor experiments has been the development of antineutrino detectors for nuclear non-proliferation purposes [15]. At short distances, these efforts have demonstrated the feasibility of using $\overline{\nu}_e$ detectors to monitor the operational state and fuel cycle of commercial nuclear reactors [16, 17], and have pursued the possibility of observing changes in the $\overline{\nu}_e$ energy spectrum over the course of the fuel cycle. Efforts are also focused on further demonstration of these purposes for a wider array of reactor types [18, 19], detection methods [19–21] and detector overburdens [18].

The National Institute of Standards and Technology (NIST) [22], Oak Ridge National Laboratory (ORNL) [23], and Idaho National Laboratory (INL) [24] operate powerful, highly compact research reactors and have identified potential sites for the deployment of one or multiple compact $\overline{\nu}_e$ detectors at distances between 4-

20 m from the reactor cores. US reactor facilities offer a unique opportunity for a search of $\overline{\nu}_e$ oscillations at very short baselines. A 5σ discovery is possible with 3 years of data taking. This note describes a proposed experiment to definitely resolve one of the outstanding anomalies in neutrino physics, make a precision study of the $\overline{\nu}_e$ spectrum, and develop the use of advanced scintillators and detectors without overburden for applications in reactor monitoring and safeguards.

II. RESEARCH REACTORS AS A LABORATORY FOR PRECISION STUDIES

The large antineutrino flux produced by nuclear power reactors has lead to such sites being the preferred venue for reactor neutrino studies over the past two decades. However, research reactors operated by scientific organizations and national laboratories possess many advantages for precision neutrino physics studies, especially at short baselines. While research reactors operate at lower powers than commercial plants, it is often possible to gain access to locations closer to the reactor core, partially compensating for any flux reduction. In addition, the geometry, core composition, and operations of research reactors offers unique advantages for a reactor experiment at very short baselines.

The primary feature of research reactors relevant to precision studies of short-baseline oscillations with a length scale of $\mathcal{O}$(m) is the core geometry and composition. While research reactor core geometries can vary considerably depending upon their design application, their spatial extent is of the order of 1m and always less than that for a power reactor. Additionally, many research reactors use fuel that is comprised primarily of Highly Enriched Uranium (HEU). Unlike the Low Enriched Uranium (LEU) or Mixed Oxide (MOX) fuel used at power reactors, there is insufficient ^{238}U present in research reactor fuel to breed substantial amounts of Pu, in particular ^{239}Pu. Accordingly, essentially all antineutrinos emitted by HEU fueled research reactors derive from ^{235}U fissions, and the core fission fractions are constant throughout a reactors operational cycle. This is in contrast to the behavior of power reactors, where Pu breeding results in time varying power contributions from ^{235}U, ^{239}Pu, and ^{241}Pu, and therefore time variation in the emitted antineutrino flux and spectrum. The near static character of research reactor antineutrino emissions is advantageous for precision studies since it substantially reduces the importance of complicated reactor evolution codes to predict fission rates throughout the reactor cycle.

Unlike power reactors, research reactors operate frequent short cycles. The resulting reactor off periods provide important opportunities for background characterization. Since research reactor duty cycles are typically no greater than 70%, there is a substantial period of reactor outage time during which to obtain direct measurement of background at such facilities. These relatively long reactor-off periods, and the fact that spent fuel is often stored close to the reactor core raises the possibility that antineutrinos emitted by long lived isotopes in the spent fuel itself might be observed.

Research reactors typically maintain detailed neutronic core models that are used to predict neutron fluxes and power densities cycle-by-cycle. This is often important as irradiation experiments that are exchanged between cycles can have a large local effect on these parameters. These models and their outputs are typically available to all users of the facility. This is potentially important for a short-baseline reactor experiment, as the core power, and hence baseline, distribution may vary slightly cycle-to-cycle. The ease with which this important information can be accessed is in contrast to the situation at commercial plants where the core models are typically proprietary, and special arrangements must be made with the plant operator and/or fuel vendor.

III. RESEARCH REACTOR SITES IN THE U.S.

The Idaho National Laboratory (INL), Oak Ridge National Laboratory (ORNL), and National Institute of Standards and Technology (NIST) operate powerful, highly compact research reactors. Each of these sites have identified potential locations for the deployment of multiple compact antineutrino detectors at distances between 4-25m from the reactor cores. In this section we describe the characteristics of each of these facilities and how a short-baseline reactor oscillation experiment can be conducted. Each site has the potential to provide excellent sensitivity to the oscillation physics of interest. Further investigation will be required to determine which site will provide the optimum combination of accessibility, background, and sensitivity.

Reactor and site parameters relevant to a short-baseline reactor oscillation experiment are summarized in Table I. The core dimensions of each of these reactors are compared in Fig. 1. The diversity of shapes and sizes reflect the different functions that these facilities were designed for. The core shape combined with the physical layout of each facility determines the range of baselines that reactor-emitted $\overline{\nu}_e$ would traverse before reaching possible detector locations. This distribution of baselines is illustrated in Fig. 2, utilizing the reactor and site information from Table I.

These facilities operate to well-planned schedules, and their central mission is to provide high reliability to many users. While the details of these operating schedules differ from facility to facility based upon maintenance and refueling needs and resource constraints, the time averaged $\overline{\nu}_e$ flux at possible near detector locations is expected to be remarkably similar at each over the next several years (Fig. 3).

Site	Power (MW_{th})	Duty Cycle	Near Detector		Far Detector	
			Baseline (m)	Avg. Flux	Baseline (m)	Avg. Flux
NIST	20	68%	3.9	1.0	15.5	1.0
HFIR	85	41%	6.7	0.96	18	1.93
ATR	120	68%	9.5	1.31	18.5	4.30

TABLE I: Reactor parameters and potential detector baselines for high power research reactors in the United States.

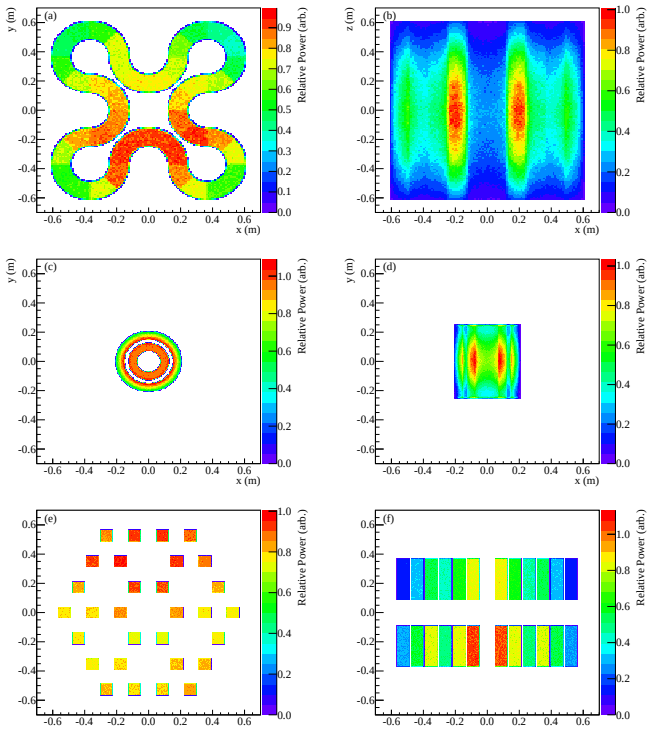

FIG. 1: Radial (left) and axial (right) core shapes and power distributions of U.S. research reactors: (a,b) ATR; (c,d) HFIR; (e,f) NIST. Note that the the ATR and HFIR power distributions can change slightly from cycle-to-cycle depending upon the material begin irradiated within those cores, whereas, as a dedicated neutron source the NIST power distribution is very similar cycle-to-cycle. Each reactor site has well established evolution codes to predict and track these distributions between and within reactors cycles.

A. The Advanced Test Reactor at INL

The Advanced Test Reactor (ATR) was designed to be a large versatile reactor for a wide variety of materials and system investigations. The ATR design exploits a unique serpentine core configuration to offer a large number of positions for testing (Fig. 1a). The core is comprised of 40 HEU fuel assemblies, approximately one third of which are replaced after each cycle. The typical residency of an assembly in the core is 2-3 operating cycles. The operating power of ATR is in the range $110 - 120$ MW_{th}, although occasionally short cycles operate as high as 200 MW_{th}.

The operating power and core power distribution vary

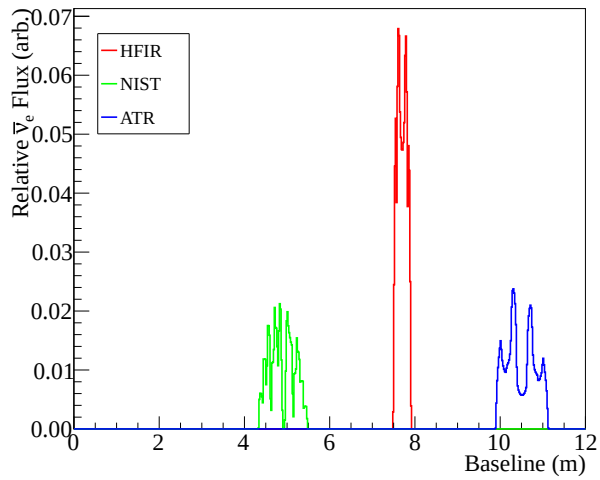

FIG. 2: (a) Baseline distributions for the ATR, HFIR and NIST research reactors, as viewed from the center of possible near detector locations. These distributions include the effect of solid angle and the core power distributions.

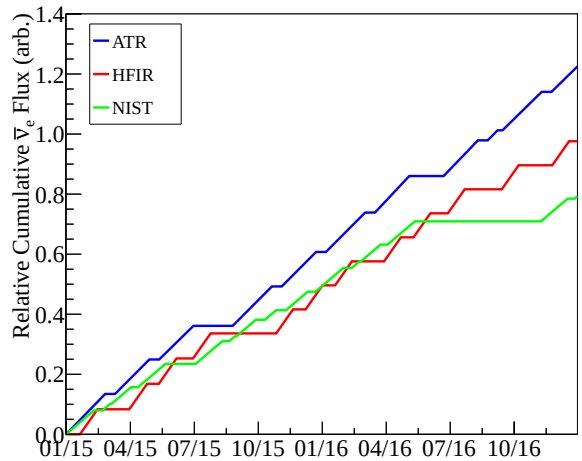

FIG. 3: Representative power histories for the ATR, HFIR and NIST reactors are used to generate cumulative flux curves for the near detector locations at these sites over a two year period beginning in 2015. Note that the NIST expects to conduct a maintenance outage of approximately 6 month length in 2016. The exposure obtained at each site is comparable over the expected duration of the experiment.

from cycle-to-cycle. The unique design of the ATR permits large power variations among its nine flux traps using a combination of control cylinders (drums) and neck shim rods. Within bounds, the power level in each corner lobe of the reactor can be controlled independently during the same operating cycle. Following each cycle, as-run analyses based on in-core measurements and reactor simulations can provide more precise power estimate for each area of the reactor.

ATR typically operates on a schedule with approximately 50-60 days at power then 15-30 days with the reactor off. There are a few exceptions to this schedule. Approximately every 2 years there is a 3-4 month outage and every 10 years a 6-8 month major outage in which internal core elements are replaced. The next such replacement outage is proposed for Apr.-Oct. 2017. ATR is scheduled to convert to LEU fuel, but this will be phased over several years and will not commence until at least 2020.

The top of the ATR reactor vessel is approximately at grade, while the center of the reactor core is located approximately 5.5 m below grade. Sub-basement levels of the facility contain potential antineutrino detector deployment locations. Potential near detector locations have been identified in the first sub-basement of the ATR building. The floor of this level is 5.8 m below grade, placing it approximately inline with the core center. At least 3.3 m of concrete and 1 m of water lie between the reactor core and this location. The distance from the core center to the closest wall in this location could be as little as 7.9 m, while the center-to-center distance from the core to the nominal detector configuration discussed below is 9.6 m. While the location is below grade, the overburden is primarily provided by building structure including a concrete floor of approximately 20 cm thickness and the exterior structure of the ATR building.

A potential far detector location has been identified in the second sub-basement of the ATR building. The floor of this level is 11.6 m below grade and at least 5.5 m of concrete and 1 m of water lie between the reactor core and this location. The center-to-center distance from the core to the nominal far detector configuration discussed below is 18.5 m. In this location overburden is primarily provided by building structure including two concrete floors of approximately 40 cm total thickness and the exterior structure of the ATR building.

B. The High Flux Isotope Reactor at ORNL

The High Flux Isotope Reactor (HFIR) was designed to provide a very high neutron flux for irradiation and isotope production applications. Multiple locations exist in the reactor for performing sample or target irradiations, some of which can be accessed during reactor operation. The HFIR core design is very compact and comprises a single fuel assembly which has two annular fuel elements (Fig. 1c). This assembly is replaced after each operating cycle.

HFIR operates at a consistent power of 85 MW_{th}, with occasional operation at lower powers during the cycle startup phase. A reactivity control system maintains this power throughout the cycle, irrespective of the irradiation experiments being performed. Given this consistent operation, it is not typical to perform as-run reactor simulation analyses cycle by cycle, although a detailed MCNP model of the core is available for this purpose .

HFIR cycles last approximately 25 days with deviations from that average being less than 36 hours. At present, 6 cycles per year are scheduled, giving a duty cycle of $\approx 41\%$. Outages between cycles have at least 14 day duration.

Potential detector deployment locations have been identified at grade level, approximately 4 m above the reactor centerline. The distance from the core center to the closest wall in the possible near detector location is as little as 5.5 m, while the center-to-center distance from the core to the nominal detector configuration discussed below is 6.7 m. The potential far detector location is located at this same grade level and provides a center-to-center baseline of 18.0 m. Overburden is provided only by the structure of the reactor building.

C. The National Bureau of Standards Reactor at NIST

The National Bureau of Standards Reactor (NBSR) at NIST is a heavy water (D_2O) cooled, moderated, and reflected, tank-type reactor that operates at a design thermal power of 20 MW. It was first critical in December 1967, and is currently licensed until July 2029. The NBSR is fueled with high-enriched uranium (HEU) with a nominal ^{235}U enrichment of 93%. The fuel is U_3O_8 in an aluminum dispersion that is clad in aluminum. As with the other sites, NIST is scheduled to convert to LEU fuel, but this will be phased over several years and currently is not expected to begin until at least 2020. The HBSR core comprises 30 HEU fuel assemblies arrayed in an approximately cylindrical geometry (Fig. 1e).

A reactor cycle is nominally 38 days. The startup usually can be accomplished in about 2 hours, after which the power is maintained at 20 MW for the remainder of the cycle. Variations in the power (about $\pm 2\%$) are minimized by the automatic movement of the regulating rod. A detailed MCNP model of the core has been used to model power distribution as a function of time and this data is publicly available. Aside from the normal operating schedule there is a longer six-month shutdown planned for mid 2016.

Multiple potential detector locations have been identified within the NBSR confinement building as well as two sites outside and adjacent to the confinement building. The shortest available baseline, allowing for an occupied space of approximately, 2.00 m wide by 3 m high by 3.5 m long, including shielding, is just outside a segment of

the biological shielding at an instrument station designated the thermal column. The thermal column consists of a heavy water tank (now filled with light water) and graphite block shielding that was previously used as a facility for intense thermal neutron beams. Due to the shielding design, fast neutron backgrounds are expected to be lower in this region than elsewhere in the confinement building. The face of the shielding to the center of the core is approximately 3.5 m. Acceptable floor loading varies from 2,000 lbs/ft^2 near the thermal column to roughly 1,000 lbs/ft^2 at the confinement wall. Access to the front face of the biological shielding in the region of the thermal column must be made available with approximately 24 hours notice to meet the needs of reactor operations., otherwise there is minimal interference between a detector at this location and normal scientific and facility operations. The far locations are both at baselines of roughly 16 m. All locations are at grade and roughly in-plane with the core. Far location have no overburden, while near locations are under roughly 50 cm concrete that comprises the structure of the confinement building.

The location of the near detector is accessible though a loading dock. The area is serviced by a 15 ton radial crane. Crane access is limited within the building due to geometrical constraints and limited floor space, thus crane activity must be coordinated with reactor operations and carried out only by approved NCNR personnel. Limited deployment at the thermal column site for prototyping purposes is possible immediately.

IV. EXPERIMENTAL STRATEGY AND PHYSICS REACH

Reactor antineutrino experiments typically utilize the Inverse Beta Decay (IBD) reaction $\overline{\nu}_e + p \rightarrow e^+ + n$ with a threshold of ∼1.8 MeV to measure the flux and energy spectrum of reactor $\overline{\nu}_e$. Liquid scintillator (LS) detectors provide a proton-rich target with high detection efficiency and good energy resolution. Rejection of backgrounds can be achieved by time-coincidence and rejection of muon-correlated triggers, as well as by other previously demonstrated methods of selection based on event topology and pulse shape discrimination.

For a U.S short-baseline reactor experiment, we propose the construction of a $\mathcal{O}(1\ \mathrm{m}^3)$-sized near detector at distances of less than 10 m and a $\mathcal{O}(10\ \mathrm{m}^3)$-sized far detector at distances of 10-20 m. These detectors will consist of optically separated functionally identical subvolumes to provide precise, reliable position resolution, consistent spectral response, and uniform background rejection capabilities. Preliminary detector and reactor parameters are listed in Table II. This experimental arrangement provides excellent sensitivity to neutrino oscillations over a broad range of mass splittings. In addition, this experiment provides precision spectral measurements of an HEU reactor core. A rendering of how such an experiment can be configured at the NIST reactor site is shown in Fig. 4.

Parameter		Value
Reactor	Power	20 MW
	Shape	cylindrical
	Radius	0.5 m
	Height	1.0 m
	Fuel	HEU
Detector	Cross-section (near)	1.2 m×0.65 m
	Cross-section (far)	1.2 m×3.25 m
	Baseline coverage (near)	2.1 m
	Baseline coverage (far)	4.2 m
	Efficiency	30%
	Proton density	$6.39\times10^{28}\ \frac{p}{m^3}$
	Position resolution	15 cm
	Energy resolution	$10\%/\sqrt{E}$
Background	S:B ratio	1
	Background shape	1/E^2 + Flat
Other	Run Time	3 years live-time
	Closest distance	3.75 m

TABLE II: Nominal detector and reactor parameters for the proposed Phase 2 experiment, in the case of deployment at NIST. The phase 1 parameters are identical with the exclusion of the far detector.

The 2-detector arrangement of the proposed experiment allows staging in 2-phases. The first phase consists of year-long measurement with the near detector, which provides a 3σ sensitivity to a broad range of oscillation parameters. The second phase consists of a three year run of both detectors, which extends the region of sensitivity and provide a conclusive test of a large portion of the oscillation parameter space at 5σ CL.

A. Sensitivity to Short-Baseline Oscillation

The sensitivity of a reactor experiment to neutrino oscillations is evaluated by comparing the detected energy spectrum to the expected one in the absence of oscillation. A radially extended detector or multiple radially extended detectors with position resolution allow a comparison as a function of baseline.

The segmented near detector will provide a precise measurement of energy spectrum at very short distances and provide sensitivity to mass splittings of order 1-10 eV^2. The far detector allows precise oscillation measurements below 1 eV^2 and the ability to observe multiple L/E oscillation periods, which increases overall sensitivity as well as enhancing the ability to distinguish between non-standard mixing models in the event that spectral distortion is observed.

The sensitivity of the proposed experiment to neutrino oscillations is evaluated by comparing the detected inverse beta decay prompt events T_{ij} in energy bin i and position bin j to the expected events M_{ij} in the absence of neutrino oscillations and in the presence of a background B_{ij}. For the purposes of these calculations, T_{ij}

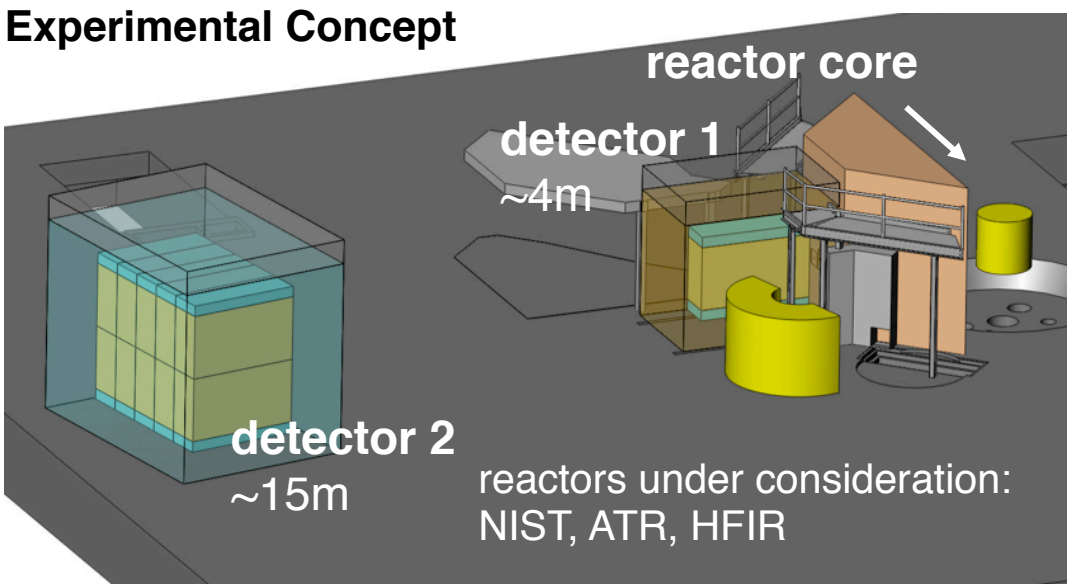

FIG. 4: A rendering of the realization of a Short Baseline Experiment at the NIST reactor site. A near detector ("detector 1") is placed as close to the reactor core as possible, while a larger far detector ("detector 2") is placed at a baseline of ≈15 m.

is taken as B_{ij} plus an oscillated version of M_{ij}. A χ^2 is used to test the hypothesis of no-oscillation and for oscillation parameter estimation in the case of either one or two additional sterile neutrino states, identically to that presented in Ref [14, 25]:

$$\chi^2 = \sum_{i,j} \frac{\left[M_{ij} - (\alpha + \alpha_e^i + \alpha_r^j)T_{ij} - (1+\alpha_b)B_{ij}\right]^2}{T_{ij} + B_{ij} + (\sigma_{b2b}B_{ij})^2} + \frac{\alpha^2}{\sigma^2} + \sum_j \left(\frac{\alpha_r^j}{\sigma_r}\right)^2 + \sum_i \left(\frac{\alpha_e^i}{\sigma_e^i}\right)^2 + \frac{\alpha_b^2}{\sigma_b^2}. \quad (1)$$

The χ^2 sum is minimized with respect to the relevant oscillation parameters and to the nuisance parameters $\{\alpha,\, \alpha_r^j,\, \alpha_e^i,\, \alpha_b\}$ characterizing the systematic uncertainties of the measurement, as described in [26]. These nuisance parameters represent the overall normalization, relative position normalization, uncorrelated energy spectrum, and background systematics. Associated bounding uncertainties of these systematics are $\{\sigma,\, \sigma_r,\, \sigma_b\} = \{100\%,\, 0.5\%,\, 10\%\}$. The uncorrelated energy spectrum uncertainties σ_e^i follow the description given in [7]. An additional uncertainty σ_{b2b} of 0.5% is added to the χ^2 to account for uncertainties in the position and energy distribution of backgrounds, which are not currently well-understood, and are likely to be uncorrelated between energy and position bins. A more pedagogical description of the χ^2 and its components is given in [14]. We note that in the 2-detector case, no special cancellation of detector systematics between near and far detectors has been assumed in these studies.

The 3+1 neutrino model with one additional sterile neutrino state and a mass splitting of ∼1 eV^2 mass is frequently used in the literature to benchmark the sensitivity of new experiments to short-baseline oscillations [9]. In keeping with this convention, we will first present the sensitivity to 3+1 neutrino oscillations for one and two detectors. The short-baseline $\overline{\nu}_e$ survival probability associated with this oscillation is described by

$$\begin{aligned} P_{ee} &= 1 - 4|U_{e4}|^2(1-|U_{e4}|^2)\sin^2\tfrac{\Delta m^2 L}{4E} \\ &= 1 - \sin^2 2\theta_{ee}\sin^2\tfrac{\Delta m^2 L}{4E}, \end{aligned} \quad (2)$$

with the oscillation amplitude $\sin^2 2\theta_{ee} = \sin^2 2\theta_{14} = 4|U_{e4}|^2(1-|U_{e4}|^2)$.

Fig. 5 shows oscillated L/E distributions assuming the existence of one sterile neutrino state for Phase 1 and Phase 2 of the experiment at three values of Δm^2. The measured L/E distributions include smearing from the finite experimental position reconstruction and the energy resolutions shown in Table II. As a second detector is added in Phase 2, the L/E coverage increases from around 2-3 m/MeV to greater than 6 m/MeV.

This increase in L/E coverage in Phase 2 translates to an increase in the observable range of Δm^2 values. In particular, at low Δm^2 values, sensitivity is greatly improved as long oscillation wavelengths are resolved within the experiment's wider L/E coverage. One can also see an increase in sensitivity for Δm^2 values covered by a one-detector arrangement. At intermediate values of Δm^2, additional L/E coverage allows the detection of multiple neutrino oscillation periods, rather than a single or partial period. The additional reach in L/E increases the ability to distinguish any observed oscillation from the null hypothesis of no-oscillation. At high Δm^2, the total number of visible oscillation periods is also increased, although the finite experimental resolution tends

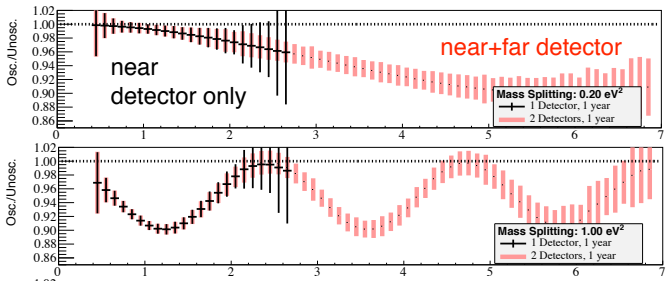

FIG. 5: Oscillated L/E distributions for 3+1 neutrino mixing assuming an oscillation amplitude of 10% and 1 year of data with one or two detectors. The default parameters described in Table II are used. In the two-detector case, the far detector active target mass is 10× that of the near detector. Error bars display statistical uncertainties only.

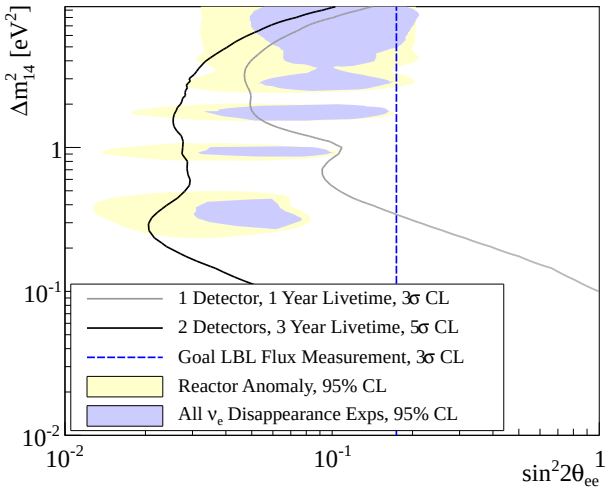

FIG. 6: Total sensitivity to 3+1 oscillations for Phase 1 (near detector only, 1 year data taking) and Phase 2 (near and far detectors, 3 years data taking). The vertical dashed line indicates the expected sensitivity of longer baseline $\overline{\nu}_e$ disappearance measurements of the reactor θ_{13} experiments. Excellent coverage of the phase space suggested by anomalous ν_e disappearance results and the "reactor anomaly" is achieved.

to damp out the oscillation effect. The resultant increase in the sensitive range of Δm^2 and θ_{14} going from Phase 1 to Phase 2 is illustrated in Fig. 6.

Oscillation sensitivity in the 3+1 case has been investigated for all of the candidate reactor sites (Fig. 7). While the near and far detector sizes and shapes are assumed to be the same, the detector baselines reflect what is realistically achievable at each site. Oscillation sensitivity is consistently high at all three reactor sites being considered, under the assumption of similar background conditions.

The increased range of L/E coverage in Phase 2 enables the observation of multiple oscillation periods for much of the suggested sterile oscillation parameter space. This extended mapping will provide significant constraints on any subdominant features in the oscillation pattern, which could result from the existence of multiple eV-scale neutrinos or other non-standard neutrino interactions. A detailed demonstration of the ability to probe 3+2 sterile neutrino oscillations, and to distinguish 3+1 and 3+2 mixing with Phase 1 and 2 is presented in [25]. The current best-fit 3+2 and 1+3+1 best-fit parameter space [27] should be accessible with the full dataset from Phase 2.

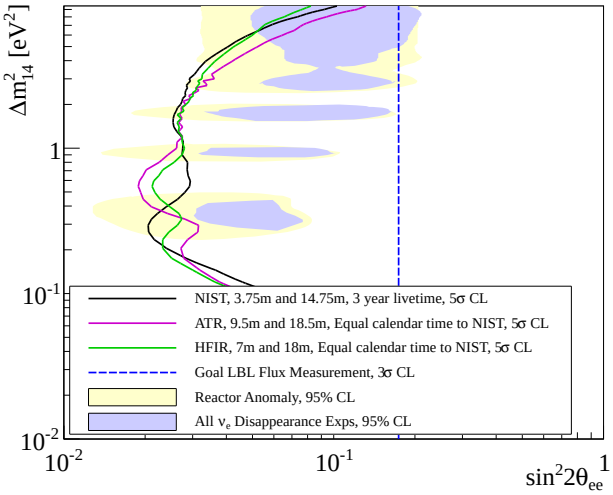

FIG. 7: Total sensitivity to 3+1 oscillations for Phase 2 for the three US research reactors under consideration. The vertical dashed line indicates the expected sensitivity of longer baseline $\overline{\nu}_e$ disappearance measurements of the reactor θ_{13} experiments.

B. Measurement of the Reactor Antineutrino Spectrum

In addition to the relative oscillation measurement performed between detectors and segments, the proposed short baseline experiment also will have the opportunity to make a precision measurement of the absolute energy spectrum of the research reactor core.

The research reactors being considered for this experiment are HEU fueled and as such their antineutrino emissions arise almost exclusively from ^{235}U fissions. A precise ^{235}U spectrum measurement could provide significant additional physics reach. Reactor antineutrino flux predictions require us to make certain assumptions about the contributing fission daughter beta decays due to incomplete nuclear data. While the final-state and nuclear corrections utilized in recent calculations are known with reasonable precision, the assumptions made regarding the character of the contributing beta decays may result in significant changes to the predicted reactor $\overline{\nu}_e$ normalization and spectrum [28]. It is not practical to measure the beta-decay shape of each isotope contributing to

the reactor antineutrino spectrum. Instead, precise reactor spectrum measurements can probe these assumptions directly, indicate the magnitude of contribution from forbidden states, and improve our confidence in reactor antineutrino flux predictions. A spectral measurement of a single fissioning isotope could improve this effort by reducing dependence upon reactor evolution codes.

A precise ^{235}U spectrum measurement could also be used in combination with LEU reactor measurements from experiments like Daya Bay [29] to provide a decomposition of the total antineutrino flux contributions from the various fissioning isotopes. This provides a cross-check on existing reactor models and is an important demonstration of the ability to use antineutrino measurements to extract reactor fissile inventory information without additional inputs like thermal power measurements.

C. Direct Measurement of Antineutrinos from Spent Fuel

During a small but significant percentage of time, the various research reactors are shut down for refueling and maintenance. During this time, while fission has largely ceased, creation of beta decay products continues in the spent fuel in the reactor and in nearby storage pools, leading to production of "spent fuel" antineutrinos. The full Phase 2 data set will contain a sizable number of such events. The measurement of the spectra and rate of these neutrinos as a function of time can provide constraints on models describing antineutrino production in reactors. At some of the candidate sites, particularly HFIR, antineutrinos created in spent fuel repositories closely adjacent to the main reactor core may also be statistically accessible. While spent nuclear fuel antineutrino statistics will be sizeable for these reactor-off periods, excellent background reduction and characterization will be the key to making a statistically significant measurement.

V. EXPECTED BACKGROUNDS AT NEAR-SURFACE RESEARCH REACTOR SITES

The sites detailed above have relatively little overburden and will require the operation of detectors close to the reactor core where both fast-neutron, neutron-capture and gamma-ray backgrounds are potentially high. Therefore, both fast neutron and muon fluxes through an unshielded detector are expected to be several orders of magnitude higher than the neutrino detection rate.

In an IBD analysis, background events can manifest in two important ways:

- *Neutron-capture Correlated Backgrounds* Events involving one or more neutrons, resulting an inter-event time correlation similar to that observed for IBD. Fast neutrons, for example, can emulate an IBD event through proton scatter and subsequent recoil followed by thermalization and delayed capture. Similarly, multiple neutrons resulting from the same cosmogenic particle may capture at different times, mimicking an IBD event.
- *Random Coincidence Uncorrelated Backgrounds* Random coincidences involving primarily either neutron recoils, neutron captures, or gamma-ray interactions can mimic an IBD event should they occur with an appropriate energy and within the average neutron capture time.

The backgrounds that will be encountered at a research reactor site fall into several broad categories, based upon their source and they way in which they manifest in a $\overline{\nu}_e$ detector.

A. Reactor Correlated Backgrounds

Locating a detector in close proximity to a reactor core is likely to introduce the special challenge of reactor correlated backgrounds that are likely to vary in time as well as space. At some locations, *e.g.*, NIST, fast neutron backgrounds are dominated by partially thermalized fission neutrons scattered from adjacent experiments. Measurements with calibrated Bonner balls yield a fast neutron flux of 2-3 cm^{-2} s^{-1} likely peaked in the 1-2 MeV range. Two segmented Fast Neutron Spectrometers (FaNS) have been developed at NIST and the University of Maryland, and will be used to further characterize fast neutron backgrounds. The FaNS detectors are capture-gated spectroscopy arrays of plastic scintillator and ^{3}He proportional counters. By demanding a coincidence between a neutron scatter in the scintillator and a neutron capture in the ^{3}He detectors, an accurate energy spectrum may be re-constructed. These detectors have been calibrated in mono-energetic neutron fields and have also been used to measure the cosmogenic neutron spectrum at the surface. Both show good agreement with MCNP predictions, including the surface spectrum up to 150 MeV. They are currently being deployed in the NIST reactor building to measure the fast neutron background *in situ*. Plans are in place to transport at least one of these detectors to the other potential sites.

An example of the gamma-ray background that could be encountered at a research reactor is shown in Fig. 8. Here, a High Purity Germanium (HPGe) gamma-ray spectrometer has been used to conduct a detailed survey of the potential NIST near detector deployment location. Backgrounds above 2.4 MeV are dominated by thermal neutron capture on reactor and experiment structural and cooling materials, yielding prompt gammas from ^{16}N and ^{57}Fe at 6.1 MeV and 7.6 MeV respectively. The reactor correlated component of the gamma-ray background is evident from the comparison of of reactor-off and reactor-on spectra is shown in Fig. 8. Notably, the ^{16}N flux shows a clear, and expected, angular dependence

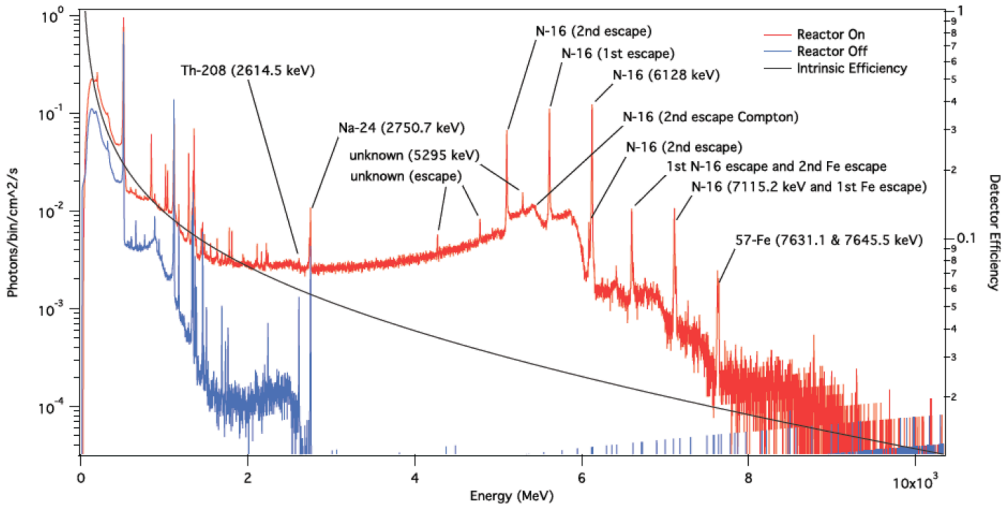

FIG. 8: Germanium spectrum taken at the potential near location at NIST during reactor on and off periods. The reactor on spectrum represents the current shielding configuration of adjacent experiments.

consistent with it originating in water filled pipes visible from certain portions of the near detector location. In general, characterization of the spatial and angular variation of such background fields will allow the design of an optimized passive shield.

B. Natural Radioactivity Backgrounds

In most $\overline{\nu}_e$ detectors, gamma, beta, and alpha decay products of the U, Th, and K decay chains present in doped scintillator, PMT glass, and metal building materials surrounding the active detector target can interact with the target scintillator, producing mainly isolated, low-energy triggers. These plentiful triggers can overlap with uncorrelated neutron interactions with the target, giving a signal-like time signature.

These radioactive background triggers can be reduced using now-standard precautions in neutrino physics, such as providing a non-scintillating buffer between PMTs and the detector target, purifying scintillator of radioactive contaminants during scintillator production, and radioassay of all detector components prior to detector construction.

C. Cosmogenic Backgrounds

Muon rates are high with respect to a typical neutrino detector, with fluxes through the active region of the detector and the shield expected to be on the order of 200 Hz and 1 kHz respectively. Additionally, the hadronic component of the cosmic ray flux will impinge the detector and shielding. As such, backgrounds from neutron spallation (muon induced or direct), muon capture, and production of radioisotopes, are of special concern. Radioisotopes such as ^{8}He and ^{9}Li have relatively long half-lives, 119 ms and 178 ms respectively, have Q-values of roughly 10 MeV, and beta-decay to neutron-unstable daughters. The decay of these isotopes can thus mimic very closely the IBD of a reactor antineutrino. Rough estimates of production rates are conservatively less than 1000 d^{-1}, indicating a challenging but tractable background. Further detailed studies are in progress. Both spallation and muon-capture can yield very high energy neutrons originating within the passive shield. Through thermalization and subsequent capture these neutrons mimic IBD events. In addition, multiple neutrons generated by the same initial cosmogenic particle can capture at different times resulting in the same timing profile as an IBD event. Monte Carlo simulation of these backgrounds is in progress.

VI. DETECTOR CONCEPTS

Performing a precision oscillation measurement within 10 m of a research reactor will be an extremely challenging task. The detector design will have to provide excellent background rejection and support precise calibrations of energy, position, and relative efficiency across the active volume. While recent reactor antineutrino experiments have used cylindrical homogenous liquid scintillator designs, the primary concept being investigated for a SBL experiment is a segmented design (Fig. 9). The basic detector segment comprises an optically isolated scintillator volume readout by PMTs at either end. There are several reasons to pursue this approach. First, the segmentation can provide intrinsic position resolution sufficient for an oscillation measurement in two axes, while relative timing and charge measurements can provide that information along the third (long) axis of the segments. Second, the segmented approach is space efficient, requiring optical readout on only 2 or 4 sides, an

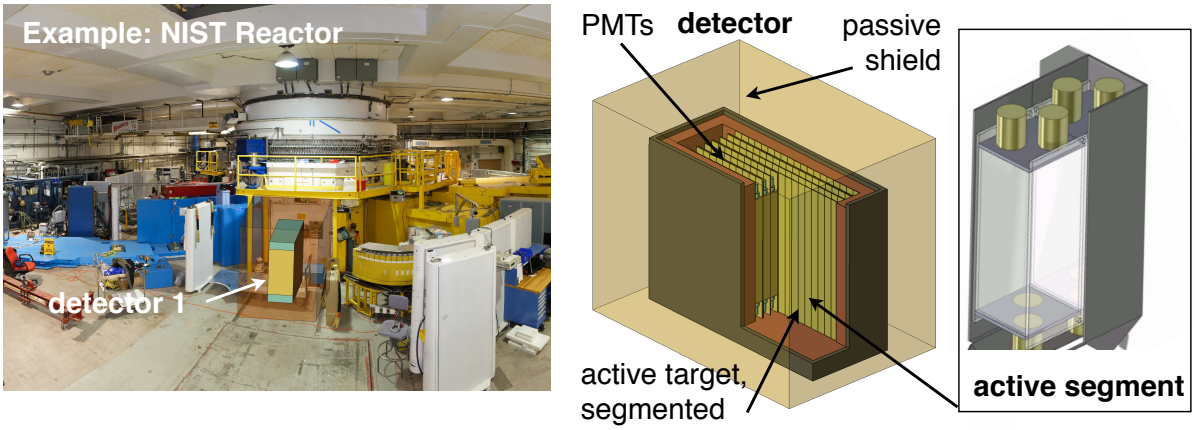

FIG. 9: Left to right: a rendering of the placement of the near detector at the potential NIST reactor site; the conceptual near detector configuration showing a segmented liquid scintillator antineutrino target and passive shielding; target segments will comprise separated scintillator volumes readout by PMTs at two ends.

important consideration in the compact spaces available at research reactors. Third, a segmented design of this type provides the opportunity to control and optimize the optical collection properties of the detector through the choice of aspect ratio and reflector material, which is potentially important for use of the Pulse Shape Discrimination (PSD) background rejection technique. Finally, segmentation provides the ability to reconstruct multi-site event topologies, e.g. identifying back-to-back 511 keV gamma rays from e^+ annihilation or multiple gamma-rays from a Gd neutron capture cascade, that could be used for signal identification or background rejection.

In addition to the intrinsic capabilities provided by segmentation, the choice of scintillator will also be important. Of course, scintillator loaded with a neutron capture agent is the target material of choice for antineutrino detection as enhances the time-coincidence signature of the positron annihilation and neutron capture resulting from the Inverse Beta Decay (IBD) interaction. The scintillator dopant increases the neutron capture cross-section, shortens the capture time, and provides a more distinct signal than the single 2.2 MeV gamma ray emitted after neutron capture on hydrogen. Both Gd and ^{6}Li doped scintillators have been used in past reactor antineutrino experiments. Neutron capture on Gd provides a distinct 8 MeV gamma ray signal above all natural backgrounds, when all of the gamma-ray energy released by the excitation cascade can be captured in the detector volume. However, the leakage of gamma rays near the detector edge can lead to inefficiencies and systematic effects, especially in compact devices like those that will be necessary for operation near a research reactor core. By contrast, the triton and alpha produced in the ^{6}Li neutron capture reaction have a very short range, resulting in a larger and more uniform detection efficiency in a compact device.

Additionally, the heavy ion products of ^{6}Li neutron capture can be identified on an event-by-event basis using PSD, providing an unambiguous indication of neutron capture. This can provide stronger uncorrelated gamma-ray rejection than Gd-doped scintillator, as well as rejection of an important multiple neutron time correlated background produced by cosmic-ray muons. Independent of neutron capture agent, PSD can also be used to identify protons recoil energy depositions caused by fast neutrons - another important source of time correlated background. The particle identification capabilities provided by this technique are likely to play an important role in providing the background rejection required for a SBL experiment.

The basic detector segment will be of rectangular or hexagonal cross section to allow a high packing density. Two construction approaches are under consideration. First, each segment could comprise a fully independent liquid containing structure made from, e.g., acrylic. Liquid filled segments could then be arranged in an array to form a detector. Good control of the segment structure manufacturing process could assist in defining similar scintillator volumes in each segment, and therefore in controlling relative segment efficiency. The drawback of this approach is that the liquid containing segment walls introduce considerable inactive material into the detector. Second, optical segmentation of a larger scintillator volume is also under consideration. This has many attractive features, including a substantial reduction in inactive material, and liquid handling complexity, and potentially increased space efficiency. A central technical challenge of this approach will be the definition of the active volume of each segment, i.e. determination of the relative efficiency of each segment.

VII. RESEARCH AND DEVELOPMENT EFFORTS

A number of R&D efforts focussed on demonstrating the viability of the proposed experiment and providing the required enabling technologies are underway. These include the development of liquid scintillators and studies of potential background rejection and calibration techniques.

Development of a suitable liquid scintillator is of central importance. A scintillator that has excellent stability, provides efficient antineutrino detection and background rejection, and has a high flashpoint is required. As mentioned above, we are considering the use of both Gd and ^{6}Li loaded scintillators. The chemistry to produce stable Gd-loaded scintillators are now well established, so our investigations on this option will focus upon optimization of PSD performance. This will be achieved through examination of a variety of fluor and wavelength shifter combinations. In addition to studies of this type, we are also developing compounds and techniques to support ^{6}Li loading in high flashpoint solvents. Significant recent progress has been made within our collaboration in this area [30, 31]. The long term stability, light yield, and neutron response of ^{6}Li loaded scintillators are under investigation.

A number of background rejection techniques are being considered. Based upon the experience of past efforts attempting reactor antineutrino detection with little overburden, we expect particle identification techniques to play an important role. In addition to the scintillator effort, PSD performance will also be considered during detector segment development. Segment geometry, reflector and PMT selection, and DAQ design will be influenced by the need for good PSD performance. The background rejection capability provided by detector segmentation is being studied via simulation. This will consider the segmentation provided by physical division of the scintillator volume and the possibility of using fast timing to provide additional position resolution. Prototype scintillator filled segments of ≈ 1 m length are under development that will allow for validation of simulations and experimental testing of various scintillator and reflector options.

Well optimized passive shielding will be needed in addition to the active background rejection techniques discussed above. In practice, the amount of shielding that can be used is limited primarily by constraints on space and weight. Fast neutrons below a few MeV and thermal neutrons can be sufficiently suppressed with careful design. For example, a factor of 10^{-6} suppression of neutrons at 1 MeV can be attained with ≈ 0.6 m of polyethylene, while hermetic boron-loaded shielding efficiently eliminates thermal neutrons. Attenuation of prompt neutron-capture gamma-rays requires high-Z materials such as lead. Optimization of such shielding based on GEANT and MCNP models, subject to realistic space and weight constraints, is currently well underway. For example, a preliminary design weighing roughly 24,000 kg and consisting of layered 5 % borated-polyethylene, lead and 5 % lithiated-polyethylene performs well in the estimated background environment at the NIST reactor site. As additional quantitative data on background fluxes at each site becomes available, site specific configurations will continue to be developed and optimized.

As with all precision experiments, calibration is an essential component of the development program. The oscillation analysis will require an excellent understanding of the relative efficiency between detector segments. Since the techniques used to determine this quantity will depend upon the detector design (e.g., optical vs physics segmentation of scintillator volume), a number of approaches are being investigated. Techniques for the precise measurement of the volume of scintillator transferred to a detector are now well established. As an alternative, we are also investigating the precision metrology of segment volumes prior to scintillator filling. We must also determine the relative antineutrino detection efficiency of the detector segments. Threshold effects can be controlled via a good understanding of relative energy scale. As in recent oscillation experiments such as Daya Bay [32], neutron capture events, various alpha and gamma-rays emissions from intrinsic radioactive backgrounds can be used for this purpose. The continuous energy spectrum provided by short-lived beta emitters, whether cosmogenic or introduced deliberately in small concentrations into the scintillator volume, could also provide a useful energy calibration source. The efficiency of positron and neutron selection cuts can be studied using external ^{22}Na and tagged neutron sources.

Measurement of the antineutrino energy spectrum emitted by an HEU fueled research reactor will require a precise absolute energy scale calibration in addition. This must account for non-linear effects arising during light production in the scintillator and in processing of signals in the detector electronics. The absolute energy scale calibration can be achieved using the background or external sources mentioned above. Beta emitters could be particularly useful in this instance, since the continuous energy spectrum can spans a wide energy range and the comparison of measured and predicted shapes can be used to test detector response models. Extensive characterization measurements of the scintillator, including measurements of the Birks parameters over a wide energy range, light absorption and re-emission characteristics, as well as dedicated measurements of electronics non-linearity, will also be required to develop such detector response models. In all of the cases mentioned above, simulation studies will be used to investigate the application of these techniques to a segmented liquid scintillator detector.

VIII. CONCLUSION

A new short baseline reactor experiment at a U.S. research reactor can provide a precision measurement of the reactor antineutrino spectrum and probe anomalous electron neutrino disappearance results through a definitive search for short-baseline oscillations. A focused research and development program is underway to characterize potential experimental locations and demonstrate that the required level of background rejection can be achieved. In addition to providing a definitive test of the "reactor anomaly", such an effort will provide a unique measurement of the ^{235}U reactor antineutrino spectrum for use in improving reactor flux predictions. Furthermore, the detection technology developed to allow operation of antineutrino detectors near-surface will provide a revolutionary reactor safeguards capability, enabling the deployment of monitoring detectors at many more locations worldwide.

[1] A. Aguilar et al., Phys. Rev. D **64**, 112007 (2001).
[2] A. Aguilar-Arevalo et al. (MiniBooNE Collaboration), Phys.Rev.Lett. **110**, 161801 (2013), 1207.4809.
[3] C. Giunti and M. Laveder, Phys.Rev. **D84**, 093006 (2011), 1109.4033.
[4] E. Komatsu et al., Astrophys. J. Suppl. **192**, 18 (2011), astro-ph/1001.4538.
[5] P. Ade et al. (Planck) (2013), 1303.5076.
[6] T. Mueller, D. Lhuillier, M. Fallot, A. Letourneau, S. Cormon, et al., Phys.Rev. **C83**, 054615 (2011), 1101.2663.
[7] P. Huber, Phys.Rev. **C84**, 024617 (2011), 1106.0687.
[8] G. Mention, M. Fechner, T. Lasserre, T. Mueller, D. Lhuillier, et al., Phys.Rev. **D83**, 073006 (2011), 1101.2755.
[9] K. Abazajian, M. Acero, S. Agarwalla, A. Aguilar-Arevalo, C. Albright, et al. (2012), 1204.5379.
[10] Y. Abe et al. (DOUBLE-CHOOZ Collaboration), Phys.Rev.Lett. **108**, 131801 (2012), 1112.6353.
[11] F. An et al. (DAYA-BAY Collaboration), Phys.Rev.Lett. **108**, 171803 (2012), 1203.1669.
[12] J. Ahn et al. (RENO collaboration), Phys.Rev.Lett. **108**, 191802 (2012), 1204.0626.
[13] *Short-Baseline Neutrino Workshop, Chicago, IL, USA, May 12-14, 2011*, URL `https://indico.fnal.gov/conferenceDisplay.py?confId=4157`.
[14] K. Heeger, B. Littlejohn, P. Mumm, and M. Tobin, Phys.Rev. **D87**, 073008 (2013), 1212.2182.
[15] A. Bernstein et al., Science and Global Security **18**, 127 (2010).
[16] N. Bowden et al., J. Appl. Phys. **105**, 064902 (2009).
[17] N. Bowden et al., J. Appl. Phys. **103**, 074905 (2008).
[18] H. Furuta et al., Nucl. Inst. Meth. **A662**, 90 (2012).
[19] D. Reyna, *Status of Current Deployments by LLNL/SNL*, AAP 2012, Honolulu, Hawaii, USA (2012), URL `http://www.phys.hawaii.edu/~jgl/AAP/AAP_2012_Agenda.htm`.
[20] S. Dazeley et al., Nucl. Inst. Meth. **A607**, 616 (2009).
[21] I. Alekseev et al. (2013), 1305.3350.
[22] NIST Center for Neutron Research, *2012 Operations Schedule* (2012), URL `http://www.ncnr.nist.gov/`.
[23] Oak Ridge National Laboratory, *The High-Flux Isotope Reactor at ORNL* (2012), URL `http://neutrons.ornl.gov/facilities/HFIR/`.
[24] ATR National Scientific Users Facility, *FY 2009 Advanced Test Reactor National Scientific User Facility Users' Guide* (2009), URL `https://secure.inl.gov/atrproposal/documents/ATRUsersGuide.pdf`.
[25] K. Heeger, B. Littlejohn, P. Mumm, and M. Tobin (2013), 1307.2859.
[26] J. Behringer et al. (Particle Data Group), Phys.Rev. **D86**, 010001 (2012).
[27] J. Kopp, P. A. N. Machado, M. Maltoni, and T. Schwetz, JHEP **1305**, 050 (2013), 1303.3011.
[28] A. Hayes, J. Friar, G. Garvey, and G. Jonkmans (2013), 1309.4146.
[29] F. An et al. (Daya Bay Collaboration), Nucl.Instrum.Meth. **A685**, 78 (2012), 1202.6181.
[30] B. Fisher, J. Abdurashitov, K. Coakley, V. Gavrin, D. Gilliam, et al., Nucl.Instrum.Meth. **A646**, 126 (2011), 1106.4458.
[31] N. Zaitseva, A. Glenn, H. P. Martinez, L. Carman, I. Pawelczak, et al., Nucl.Instrum.Meth. **A729**, 747 (2013).
[32] F. An et al. (Daya Bay Collaboration), Chin. Phys. **C37**, 011001 (2013), 1210.6327.